doi:10.1016/j.jmb.2006.07.011 J. Mol. Biol. (2006) 362, 347–354

JMB

Available online at www.sciencedirect.com

ScienceDirect

ELSEVIER

Quaternary Structure of a Mature Amyloid Fibril from Alzheimer's Aβ(1-40) Peptide

Carsten Sachse[1,2], Chen Xu[2], Karin Wieligmann[1], Stephan Diekmann[1] Nikolaus Grigorieff[2]* and Marcus Fändrich[1]*

[1]*Leibniz Institut für Altersforschung, Fritz-Lipmann Institut, 07745 Jena, Germany*

[2]*Brandeis University, Rosenstiel Basic Medical Sciences Research Center, MS 029, Waltham MA 02454-9110, USA*

**Corresponding authors*

Amyloid fibrils are fibrous polypeptide aggregates that can be formed *in vitro* and under pathologic conditions, such as in type II diabetes, Alzheimer's and Creutzfeldt-Jakob diseases. Using a range of biophysical techniques including electron microscopy we have analysed the quaternary structure of a mature amyloid fibril formed from the Aβ(1-40) peptide from Alzheimer's disease. We find that the analysed fibril is discernibly polar and represents a left-handed helix consisting of two or three protofilaments. These are organised in a manner so that the cross-section is, under the present resolution conditions (2.6 nm), S-shaped. In the cross-section, each protofilament can accommodate two β-strands, suggesting that each protofilament contains two cross-β-sheets. These data shed new light on the way in which Aβ(1-40) and the protofilaments formed from this peptide are organised within the mature fibril.

Keywords: aggregates; neurodegeneration; protein folding; prion

Introduction

Amyloid fibrils occur inside the human body, often associated with aging or neurodegenerative conditions.[1] One example is Alzheimer's disease. Although the pathogenic role of Aβ fibrils or aggregates is, for the Alzheimer's disease, still under debate, increasing evidence suggests that Aβ acts in a cascade of events resulting ultimately in neuronal degeneration and other Alzheimer-specific, phenotypic alterations.[2] Aβ occurs inside the human brain in peptide isoforms of different length. The 40 residue peptide Aβ(1-40) represents the most abundant isoform in the cerebral cortex of Alzheimer patients,[3] while the minor species Aβ(1-42) shows a significant disease-associated increase.[4] *In vitro*, Aβ(1-40) can form aggregates of different structure, including protofibrils and mature fibrils.[4,5] The latter are end products of fibril formation, and they are defined by a long, straight and often twisted overall structure, and also by their strong affinity for Congo red. Mature fibrils can occur in different morphologies, varying in thickness, twist and protofilament organisation.[5–7]

In all cases, amyloid fibrils are defined by the presence of the same basic type of polypeptide structure, termed the cross-β conformation.[8] This structure is invariably the same, irrespective of the sequence constructing the fibrils or the disease states under which they occur.[1,8] *In vitro*, amyloid-like fibrils can be formed by many natural polypeptide chain sequences, even though these are not known to do so *in vivo*, such as apomyoglobin or several polyamino acids.[1,9,10] These and other observations resulted in the proposal that amyloid fibrils represent a generic polymer state of the polypeptide chain.[1] Several models have been put forward to propose conformational arrangements of the polypeptide chains in the fibril that could be the same for different polypeptide sequences.[8,11–13] In addition, small peptides, which form amyloid-like contacts within microcrystalline arrays have been suggested as amyloid model structures.[14,15]

Aβ peptide fibrils have been studied previously with a range of techniques, including nuclear magnetic resonance (NMR). Using solid-state NMR (ss-NMR), the structure of the single Aβ(1-40) peptide in the fibril and the nature of direct peptide–peptide contacts were explored.[6,7,17,18] Another model was determined for Aβ(1-42) by hydrogen/deuterium-exchange NMR.[16] For the Aβ(1-40) or Aβ(1-42) peptides it suggested a U-

Abbreviations used: 3D, three-dimensional; CEM, cryo-electron microscopy; ss-NMR, solid-state nuclear magnetic resonance.

E-mail addresses of the corresponding authors: niko@brandeis.edu; fandrich@fli-leibniz.de

turn-shaped conformation in the fibril, consisting of two β-strands and an intervening loop. However, different studies assign the loop region to slightly different residues.[6,13,16–18] Furthermore, different peptide conformations seem to exist in the fibrils and some fibril samples contain the peptide in a 2:1 molar ratio of conformations.[7] Previously, cryo-electron microscopy (CEM) enabled reconstructions of amyloid fibrils from insulin, SH3-domain or prion protein.[19–21] Here, we have analysed the quaternary structure of one such fibril by CEM and other structural techniques.

Results

Morphological homogeneity of the fibril samples used in the present analysis

Biophysical analysis of amyloid fibril samples is often complicated by the fact that these samples contain a large diversity of fibril morphologies.[5,6] As an initial step we carried out a screen of different conditions of fibril formation of Aβ(1-40) peptide and their effect on the structural homogeneity of these samples. This screen resembled a crystallisation trial and established that incubation in 50 mM sodium borate (pH 9.0), leads to the population of a single fibril species that is highly abundant (Figure 1(a)). This fibril morphology accounts for 92% of the fibrils longer than 300 nm (Figure 1(b)) and it is defined by a width of approximately 20.5 nm and a rather straight and unbranched appearance (Figure 1(a)). However, the individual fibrils of this morphology can differ in length and in the distance of adjacent cross-overs. As examined in more detail below, these cross-overs reflect a periodic twist of the overall fibril structure.

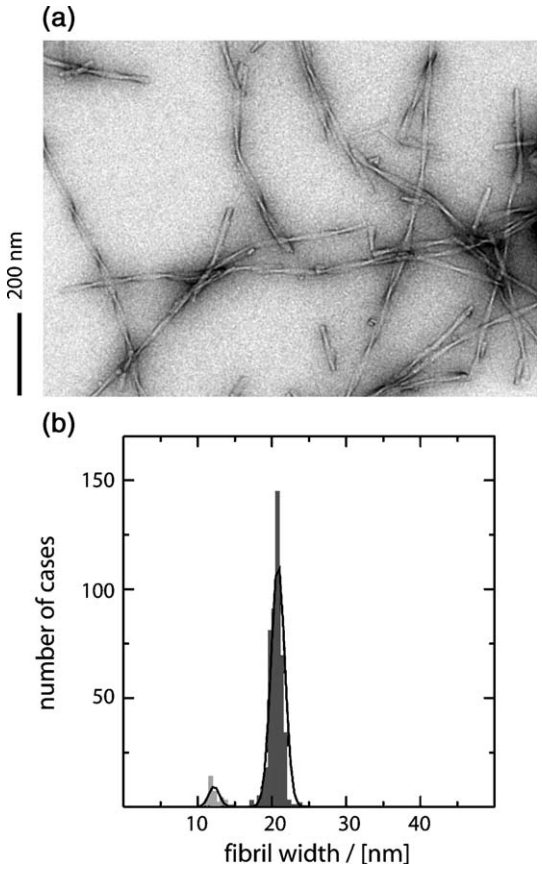

Figure 1. Structural homogeneity of the fibril sample. (a) Images of fibrils in negative stain (2% (w/v) uranyl acetate). (b) Histogram of the fibril width distribution from 500 cross-overs (negative stain) measured from fibrils longer than 300 nm. Dark gray bars, main morphology accounting for 92% of the fibrils; light gray, minor morphology corresponding to 8% of the fibrils.

Amyloid nature of the fibrils present in solution

Far-ultraviolett circular dichroism spectroscopy demonstrates the presence of a β-sheet conformation (Figure 2(a)). Attenuated total reflectance Fourier-transform infrared spectroscopy shows narrow amide I and II maxima centred at 1628 cm^{-1} and 1549 cm^{-1} (Figure 2(b)). These properties are highly characteristic for aggregated or amyloid-like β-sheets which were found to lead, within the amide I′ region, to absorption maxima between 1610 cm^{-1} to 1630 cm^{-1}.[22] When fibrils are uniaxially aligned and exposed to X-ray irradiation they produce an anisotropic diffraction pattern with a meridional spacing of 4.76 Å (Figure 2(c)). This reflection spot indicates the distance of two hydrogen-bonded β-strands of the same β-sheet. Its meridional orientation demonstrates, therefore, that the strands of the sheet run transversely to the main fibril axis. This arrangement is termed a cross-β structure.[8] The fibrils have strong affinity for aggregate-specific dyes, such as Congo red or thioflavin-T, and their Congo red bound forms give rise to discernible apple-green birefringence when viewed in a polarising microscope with crossed polarisers (Figure 2(d) to (e)). Taken together, these characteristics establish firmly the presence of the amyloid-like and mature properties of these fibrils.

Overall topology of the reconstructed fibril

Platinum shadowing of the fibrils reveals that the periodicity and the cross-over structure of the fibrils are associated with a fibril supertwist (Figure 3(a)). This twist is left-handed in all cases. The same result was obtained with atomic force microscopy (Figure 3(b)). A left-handed fibril twist has been observed in most, if not all, twisted amyloid fibril morphologies examined to date[5,20] and also previously in fibrils formed from Aβ(1-40) peptide. The direction of the twist is thought to reflect the generic left-handed twist of β-sheet structures.[20,22] To analyse the fibril quaternary structure in more detail by three-dimensional (3D) reconstruction, fibrils were embedded in vitreous ice and analysed by CEM (Figure 3(c)). From 1533 segments (105 nm length) we obtained a

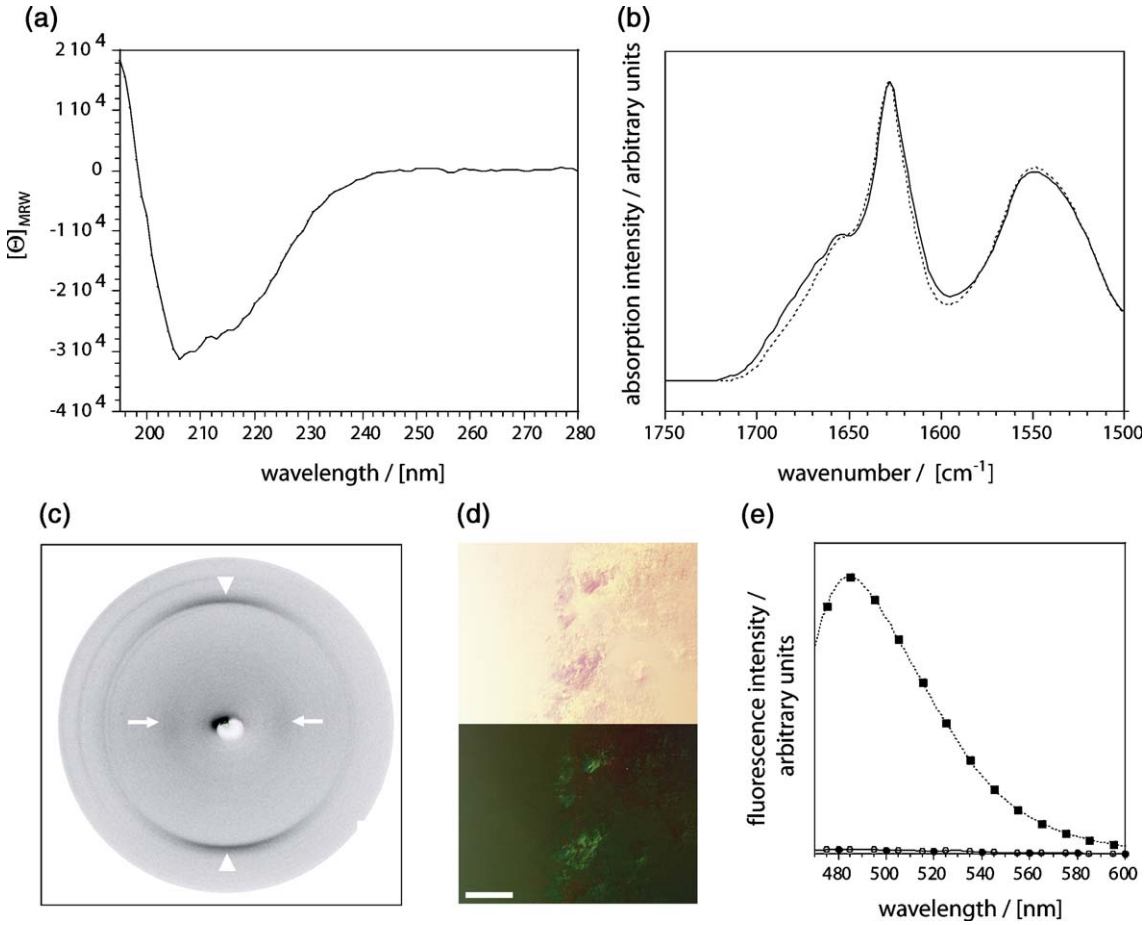

Figure 2. Amyloid properties of the fibrils. (a) Far-ultraviolett circular dichroism spectrum of Aβ(1-40) fibrils. The mean residue weight ellipticity is given in cm^2 $dmol^{-1}$. (b) Amide I region of the infrared spectrum of the fibril sample after seven days (dotted line) and 14 days of incubation (continuous line) at 20 °C. (c) X-ray diffraction image. Arrowheads show the sharp meridional main-chain spacing (4.76 Å); arrows show the diffuse equatorial side-chain reflection (inner rim 9.6 Å; outer rim 10.1 Å). (d) Polarising microscopy images of fibril samples stained with Congo red: top, bright field; bottom, dark field; the scale bar represents 100 μm. (e) Fluorescence spectra of Aβ fibrils (black squares) or freshly dissolved, disaggregated peptide (black circles) with thioflavin-T, or of thioflavin-T alone (open circles).

density map at about 2.6 nm resolution (Figures 3(d) and 4; Table 1). The average cross-over distance in this data set is 135 nm, measured from raw cryo images (Figure 3(e)). Besides the cross-over periodicity, however, no subunit repeat is recognisable in the raw images (Figure 3(c)) and in the reconstruction (Figure 3(d)), such as the 2.7 nm repeat found for the SH3-domain amyloid.[19] Furthermore, the present fibrils do not reveal a hollow core or ring-like cross-section described for other amyloid fibrils.[19,23] Instead, these fibrils are ribbon-like in shape (Figure 3(d)) and the cross-overs show clear polarity (Figure 3(c)). Comparison of projections of the reconstructed fibril with the original data shows good correspondence (Figure 5).

Interpretation of the density map

The fibril cross-section comprises three core regions of higher density that are similar in size and shape (Figure 6(a)). Each core region is approximately 8 nm long and 3.5 nm wide and may represent an individual protofilament (see below). Within the cross-section, the core regions are joined by end-to-end contacts resulting in an appearance of the fibril cross-section that resembles a stretched version of the letter S (Figure 6(a)). The two outer core regions differ in their morphology from that of the central core region. The latter has a somewhat more buried surface area due to its contacts with the two peripheral core regions, while the peripheral core regions are more exposed and contact only one other core region each.

To interpret the density we have compared our fibril reconstruction with the dimensions of the single peptide and also with possible structural models of amyloid fibrils (Figure 6(b) to (f)). This shows that a fully extended Aβ chain or generic amyloid fibril models from recent publications[8,11–13] do not easily fit our structure. By contrast, the size and shape of the core regions of our cross-section show good agreement with the dimensions of a recently published structural model of residues 9–40 of the Aβ peptide in a U-turn-like conformation (Figure 6(b)). When filtered to 2.6 nm resolution

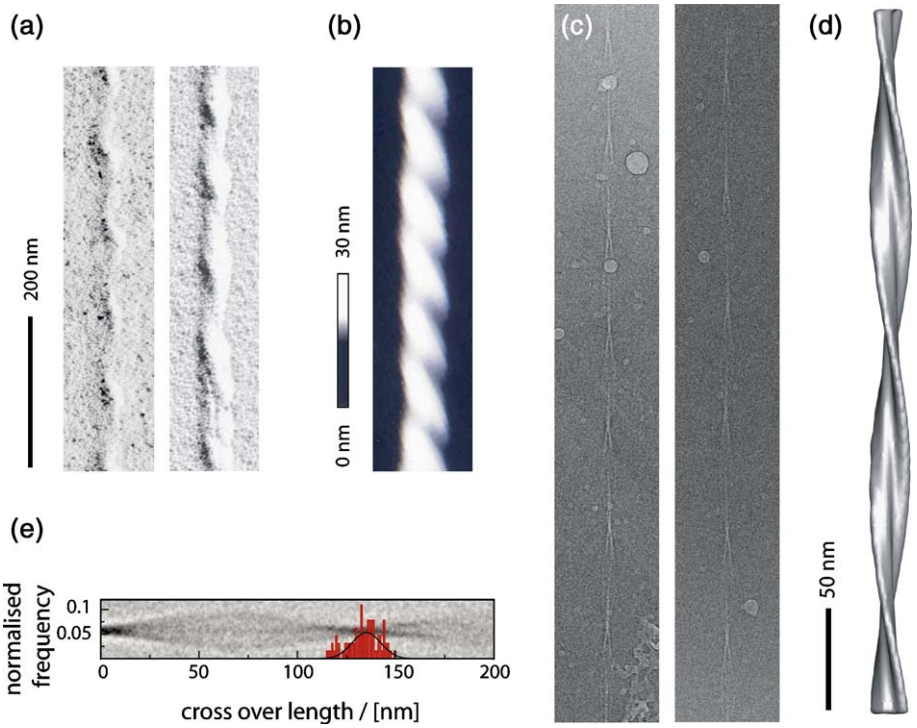

Figure 3. Quaternary structure of the fibril. (a) Electron micrograph of a fibril after platinum shadowing and (b) atomic force microscopic image of the fibril showing the left-handed overall twist. (c) CEM images of a fibril frozen in vitreous ice. (d) Side view of the reconstructed fibril. (e) Histograms of one cross-over length superimposed onto manually aligned and averaged CEM images. The red bars of the histogram are fitted with a Gaussian curve.

such arrangements lead to an overall dimension of 3 nm×7.3 nm. This size is in close correspondence with the size of the core regions described above. However, 20% of the residues of the peptide are not included in this model and the full-length peptide might require more space than indicated by the model. Hence, there is room in our 3D reconstruction to accommodate two or, depending on the conformation of the eight residues missing in the peptide model, three protofilaments (see below). It is of note that although a turn-like peptide structure fits our density map particularly well, the resolution of our reconstruction does not exclude other peptide conformations that do not feature a turn but, for example, have a structure extending across two core regions. By contrast, our data are inconsistent with an arrangement of two or four turn-like Aβ molecules that interact through their β-sheet regions as suggested for other Aβ(1-40) peptide fibrils.[6,16,18] None of the three core regions is large enough to accommodate such an arrangement. It is possible, however, that other fibril morphologies described elsewhere[5] are more consistent with some of the previously proposed arrangements of peptides.

Although our fibril reconstruction puts clear constraints on a number of previously proposed fibril models, it is not possible to discern at the current resolution of 2.6 nm, the number of protofilaments making up a fibril. Therefore, the density may accommodate two peptides in cross-section with the peptides contacting each other in the fibril centre. This interpretation would leave

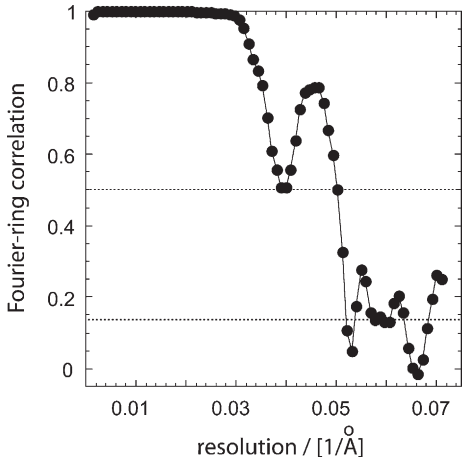

Figure 4. Resolution of the reconstruction. The Fourier-ring correlation of two independently reconstructed volumes from two halves of the data set indicates a dip at about 2.6 nm resolution. The reconstruction was low-pass filtered to this resolution.

Table 1. Fibril reconstruction statistics

Total length of non-overlapping segments (nm)	14,957
Number of fibrils	52
Number of segments	1533
Segment size (nm)	105
Average cross-over (nm)/repeat distance (Å)	135/4.76
Pixel size on the specimen (nm)	0.7

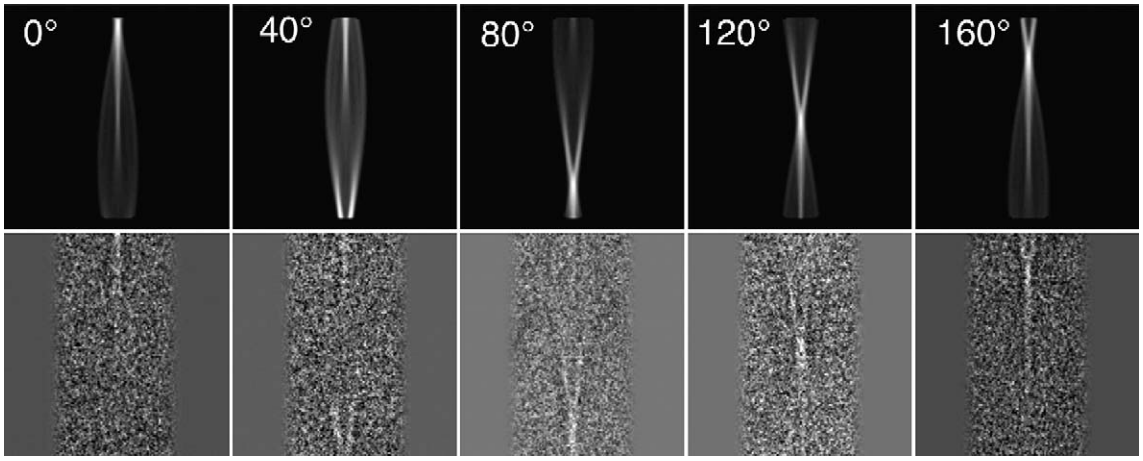

Figure 5. Comparison of projections of the fibril reconstruction with the original data. Projections of the fibril reconstruction at different axial rotation angles (top row) show good agreement with the raw images (bottom row), indicating that the reconstruction is consistent with the data.

sufficient room to accommodate the additional 20% of residues not included in the NMR structure. Alternatively, each of the three core regions may accommodate one peptide in cross-section, giving rise to three protofilaments. A determination of the precise number of protofilaments has to await a reconstruction at higher resolution. Based on the good fit of the turn-like peptide structure containing two juxtaposed β-strands, however, we suggest that the central spine of each protofilament is formed by two β-sheets in which the backbone hydrogen bonds are oriented parallel to the main fibril axis. This assembly is consistent with the cross-β structure revealed by X-ray analysis (see above).

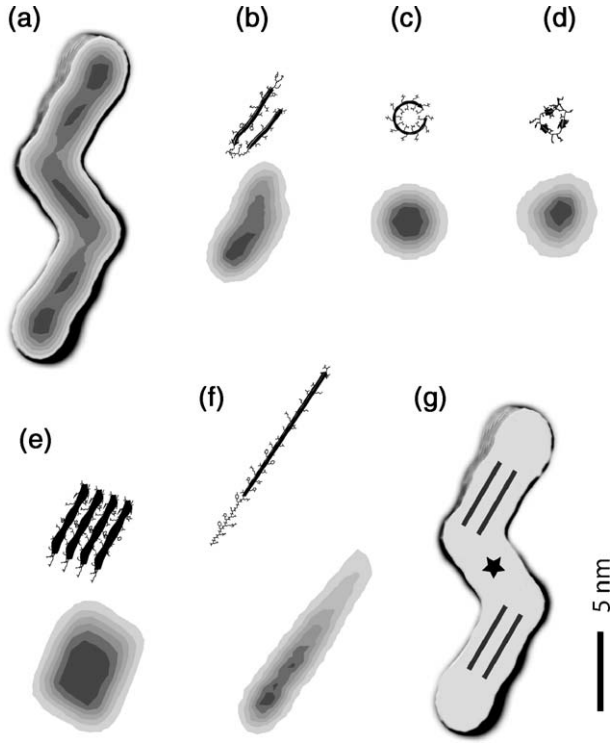

Figure 6. Interpretation of the fibril cross-section. Comparison of the observed fibril cross-section (a) with the dimensions of atomic models and their simulated densities at 2.6 nm resolution: (b) the ss-NMR Aβ model of residues 9–40; (c) nanotube;[16] (d) β-helix from pectate lyase superimposed with residues 15–36 from Aβ(1-40)[17]; (e) four-sheet protofilament model superimposed with residues 12–42;[15] and (f) fully extended Aβ(1-40) peptide. (g) Fit of the fibril cross-section with two β-strands represented as bars, per core region. The star indicates the central core region of uncertain molecular identity.

Discussion

The present analysis of the quaternary structure of a single amyloid fibril morphology formed from Aβ(1-40) peptide has been facilitated by preparation of samples containing a narrow distribution of fibril morphologies suitable for 3D reconstruction. The observed morphology corresponds to Aβ(1-40) fibril morphologies described recently.[5]

The density map derived here has been interpreted by comparison with structural models of Aβ peptide proposed previously (Figure 6), which lend support for a turn-like peptide conformation. Previous evidence for such a conformation has come from cross-linking,[26] NMR[6,16–18] and observations that a lactam-enforced U-turn leads to accelerated fibril nucleation.[27] Depending on whether or not the central core region contains a separate protofilament, the present reconstruction can be fit with two or three peptide units in cross-section. The twist and amount of buried surface area of the central core region differ from those of the two outer core regions. These differences imply possible conformational differences between the central and peripheral protofilaments. Such an interpretation would be consistent with literature data obtained from ss-NMR, hydrogen exchange and proteolysis that suggest that Aβ peptide can form fibrils in which the peptide is present in sterically non-equivalent positions.[7,24,25] However, NMR reports also fibril species that show only a single peptide conformation. This would be more consistent with a fibril

containing only two protofilaments. Which of these different possibilities is realised in the present fibrils has to await more detailed structural information about the fibril, and in particular, about the central core region.

In contrast, the present data clearly show that juxtaposed protofilaments do not interact, in this fibril, through a non-covalent packing of the β-sheet regions from different protofilaments. Such an arrangement was suggested previously for other fibril morphologies.[6,18] Instead, the present fit of the protofilament structure with a turn-like peptide conformation and two β-sheets implies, for our observed fibril morphology, that the interaction surfaces of juxtaposed protofilaments are formed by interactions occurring at the terminal ends of the β-strands or in loop regions protruding from these strands. Based on the location of the β-strands in the sequence[6] these interaction surfaces are formed from the peptide N and C termini as well as from the loop-region intervening the two β-strands, which contains approximately residues 21–29. Interestingly, all known natural variants of Aβ, most of which are associated with familial forms of the disease,[4] show variations in precisely these regions of the peptide. Furthermore, residues 21–29 can be particularly sensitive to proline scanning mutagenesis[28] and often these residues are buried and highly protected against hydrogen exchange.[24]

Besides the 40 residue peptide isoform Aβ(1-40), Aβ peptide can occur also with a longer main-chain length, for example as the 42 residue peptide Aβ(1-42). The latter peptide has been suggested to adopt, within the fibril, also a turn-like conformation consisting of two β-strands,[16,17] but CEM reconstructions of such fibrils have not been published. A recent analysis of fibril projections, however, suggests that this peptide can form fibrils where four turns are arranged side-by-side when viewed in cross-section.[16] These fibril models resemble a morphology proposed for Aβ(1-40)[6] and the major difference of the two peptides may arise merely from the higher intrinsic aggregation propensity of Aβ(1-42).[4]

In-depth knowledge about the quaternary structure of the fibrillation end product will be a prerequisite for developing a more thorough understanding of the principles governing the architecture and the formation of such amyloid fibrils, in particular, when considering the potentially more harmful precursors of mature structures.[4]

Materials and Methods

Sample preparation

Synthetic Aβ(1-40) peptide was obtained from Bachem. The peptide was mostly reduced (>95%) as shown by reverse phase chromatography. Fibrils were formed at 1 mg/ml concentration by incubation in 50 mM sodium borate (pH 9.0), at 20 °C for a minimum of 24 h.

Circular dichroism (CD) spectroscopy

The far-ultraviolett CD spectra were recorded on a JASCO J-720 spectropolarimeter using quartz cells (Hellma) of 1.0 mm path length that were optimised for polarimetrical measurements. Peptide concentrations were determined using the Coomassie Plus™ kit (Pierce).

Fourier-transform infrared spectroscopy

Infrared spectra were recorded using a Bruker Tensor 27 spectrometer (Bruker Optik, Ettlingen, Germany) equipped with a BIO-ATR II cell and a LN-MCT Photovoltaic detector. Spectra represent the sum of 40 scans after reference subtraction and one times zero-filling. They were recorded at room temperature and at a resolution of 4 cm^{-1}. The peptide was dissovled at 2 mg/ml concentration in pure water and the pH was adjusted with NaOH to pH 9.0.

Thioflavin-T fluorescence spectroscopy

All samples were recorded in 50 mM sodium borate buffer (pH 9.0). Aβ peptide or final fibril concentrations were 0.05 mg/ml and the thioflavin-T concentration was always 20 μM. All fluorescence measurements were carried out at room temperature and by using a SHIMADZU RF-5301PC fluorimeter (Jena, Germany). Emission spectra were recorded between 460 nm and 600 nm (emission slit setting 5) whilst exciting at 450 nm (emission slit setting 3).

Congo red staining and polarising microscopy

The test for apple-green birefringence was performed by drying 50 μl aliquots of a fibril suspension (1 mg/ml) on a glass slide. The fibrils were stained using a freshly filtered Congo red solution (0.1% (w/v) in water). Excessive and non-specific Congo red stain was removed by washing in water and ethanol. Samples were analysed using a LEICA DM/DR 450× polarisation microscope (Bensheim, Germany).

X-ray fibre diffraction

X-ray specimens were prepared by drying of 50 μl of a 10 mg/ml solution of Aβ(1-40) fibrils between two wax-filled glass capillaries. The X-ray images were recorded with an exposure time of 30 min and a sample–detector distance of 325 mm.

Atomic force microscopy

For atomic force microscopy analysis, samples were diluted with ultrapure water to a final concentration of 1 μg/ml. Aliquots (10 μl) of the diluted solution were placed on a freshly cleaved mica plate (Plano, Wetzlar, Germany). After 2 min, the mica was washed with ultrapure water and dried in a dessicator for at least 2 h. Tapping mode atomic force microscopy images were recorded using a Nanoscope III Multi Mode Workstation (Digital Instruments, Santa Barbara, USA), equipped with a lateral scanner (140 μm) and NCH silicon point-probes (force constant 32 N/m to 60 N/m; Nanoprobes, Neuchatel, Switzerland). We used frequencies of 298 kHz

to 366 kHz, drive amplitudes between 150 mV and 300 mV and scan rates of 1 Hz to 2 Hz.

Electron microscopy

For platinum shadowing, fibrils were unidirectionally shadowed with platinum-iridium mixtures using elevation angles of 20° to 35° and analysed using a Philips EM 400 T microscope. CEM samples were prepared as described elsewhere.[29] Vitrified specimens were imaged in a Philips CM12 transmission electron microscope at 120 kV using a magnification of 60,000x, low-dose conditions and a temperature of –180 °C. Micrographs were recorded at an underfocus of 2.0(±0.2) μm.

Image processing

Negatives were digitised using a Zeiss SCAI flatbed scanner at a raster size of 7 μm and further averaged to give a final pixel size on the specimen of 0.7 nm. The defocus of each micrograph was confirmed using CTFFIND.[30] Non-overlapping and straight fibrils were selected and cropped into rectangular boxes. Filaments were cut into segments of 150×150 pixels and masked by a cosine-edged rectangle. Further image processing was carried out with the SPIDER software package[31] using the Iterative Helical Real Space Reconstruction method.[32] Out-of-plane tilt was corrected by maximally ±12°. For the reconstruction we imposed helical symmetry with a subunit repeat of 4.76 Å, and according to a cross-over distance of 135 nm, a rotation of 0.63° per peptide. The reconstruction was low-pass filtered to a resolution of 26 Å, corresponding approximately to the first zero of the contrast transfer function of the electron microscope at an underfocus of about 2.0 μm. A 2-fold symmetric fibril was obtained with the additional insertion of each mirror image (along the fibril axis) into the reconstruction. Similar to a previous analysis of insulin amyloid fibrils[20] the raw data contained features that might indicate fibril asymmetry either owing to noise and deviation from a strict helical architecture or possibly to subtle features in the fibril, including small local bends. Although the statistical significance of these deviations was marginal, their possible effect was explored in a reconstruction of an asymmetric density map (not shown). This reconstruction retained major features of the one shown in Figures 3(d) and 5(a), such as overall size and shape of fibril (Figure 3(d)) and cross-section (Figure 6(a)), and the partitioning of the cross-section into three core regions and similar dimensions as in Figure 3(a). The central core region showed a more uneven density. While the possible relevance of such an asymmetric fibril reconstruction remains to be established, the present interpretation of the fibril architecture is not affected. The quality of the reconstruction was assessed using the average Fourier ring correlation between density slices of one pixel thickness along the helix axis from two independently reconstructed volumes. The two reconstructions were obtained by dividing the whole data set in two halves and carrying out two truly independent refinement cycles until convergence.[33] Further reconstruction details are given in Table 1.

Molecular modelling

The peptide structures were modelled according to the literature[6,8,11–13] using the program Insight (BIOSYM/Molecular Simulations) and Xfit.[34] Images were generated with the help of the Chimera Visualisation System.[35]

Acknowledgements

M.F. is supported by grants from the Bundesministerium für Bildung und Forschung (BMBF, BioFuture) and from the Deutsche Forschungsgemeinschaft (DFG). N.G. gratefully acknowledges financial support from the National Institutes of Health (grant 1 P01 GM-62580), and the Humboldt Foundation. The authors acknowledge the technical assistance from J. Chen, M. Kittler, M. Nache and K. Buder.

References

1. Dobson, C. M. (2003). Protein folding and misfolding. *Nature*, **426**, 884–890.
2. Mattson, M. P. (2004). Pathways towards and away from Alzheimer's disease. *Nature*, **430**, 631–639.
3. Mori, H., Takio, K., Ogawara, M. & Selkoe, D. J. (1992). Mass spectrometry of purified amyloid beta protein in Alzheimer's disease. *J. Biol. Chem.* **267**, 17082–17086.
4. Caughey, B. & Lansbury, P. T. (2003). Protofibrils, pores, fibrils, and neurodegeneration: separating the responsible protein aggregates from the innocent bystanders. *Annu. Rev. Neurosci.* **26**, 267–298.
5. Goldsbury, C. S., Wirtz, S., Muller, S. A., Sunderji, S., Wicki, P., Aebi, U. & Frey, P. (2000). Studies on the in vitro assembly of a beta 1-40: implications for the search for A beta fibril formation inhibitors. *J. Struct. Biol.* **130**, 217–231.
6. Petkova, A. T., Ishii, Y., Balbach, J. J., Antzutkin, O. N., Leapman, R. D., Delaglio, F. & Tycko, R. (2002). A structural model for Alzheimer's beta -amyloid fibrils based on experimental constraints from solid state NMR. *Proc. Natl Acad. Sci. USA*, **99**, 16742–16747.
7. Petkova, A. T., Leapman, R. D., Guo, Z., Yau, W. M., Mattson, M. P. & Tycko, R. (2005). Self-propagating, molecular-level polymorphism in Alzheimer's beta-amyloid fibrils. *Science*, **307**, 262–265.
8. Sunde, M., Serpell, L. C., Bartlam, M., Fraser, P. E., Pepys, M. B. & Blake, C. C. (1997). Common core structure of amyloid fibrils by synchrotron X-ray diffraction. *J. Mol. Biol.* **273**, 729–739.
9. Fändrich, M., Fletcher, M. A. & Dobson, C. M. (2001). Amyloid fibrils from muscle myoglobin. *Nature*, **410**, 165–166.
10. Fändrich, M. & Dobson, C. M. (2002). The behaviour of polyamino acids reveals an inverse side chain effect in amyloid structure formation. *EMBO J.* **21**, 5682–5690.
11. Li, L., Darden, T. A., Bartolotti, L., Kominos, D. & Pedersen, L. G. (1999). An atomic model for the pleated beta-sheet structure of Abeta amyloid protofilaments. *Biophys. J.* **76**, 2871–2878.
12. Perutz, M. F., Finch, J. T., Berriman, J. & Lesk, A. (2002). Amyloid fibers are water-filled nanotubes. *Proc. Natl Acad. Sci. U S A*, **99**, 5591–5595.
13. Guo, J. T., Wetzel, R. & Xu, Y. (2004). Molecular modeling of the core of Abeta amyloid fibrils. *Proteins: Struct. Funct. Genet.* **57**, 357–364.

14. Jaroniec, C. P., MacPhee, C. E., Bajaj, V. S., McMahon, M. T., Dobson, C. M. & Griffin, R. G. (2004). High-resolution molecular structure of a peptide in an amyloid fibril determined by magic angle spinning NMR spectroscopy. *Proc. Natl Acad. Sci. USA*, **101**, 711–716.
15. Nelson, R., Sawaya, M. R., Balbirnie, M., Madsen, A. O., Riekel, C., Grothe, R. & Eisenberg, D. (2005). Structure of the cross-beta spine of amyloid-like fibrils. *Nature*, **435**, 773–778.
16. Lührs, T., Ritter, C., Adrian, M., Riek-Loher, D., Bohrmann, B., Dobeli, H. *et al.* (2005). 3D structure of Alzheimer's amyloid-beta(1-42) fibrils. *Proc. Natl Acad. Sci. USA*, **102**, 17342–17347.
17. Masuda, Y., Irie, K., Murakami, K., Ohigashi, H., Ohashi, R., Takegoshi, K. *et al.* (2005). Verification of the turn at positions 22 and 23 of the beta-amyloid fibrils with Italian mutation using solid-state NMR. *Bioorg. Med. Chem.* **13**, 6803–6809.
18. Petkova, A. T., Yau, W. M. & Tycko, R. (2006). Experimental constraints on quaternary structure in Alzheimer's beta-amyloid fibrils. *Biochemistry*, **45**, 498–512.
19. Jimenez, J. L., Guijarro, J. I., Orlova, E., Zurdo, J., Dobson, C. M., Sunde, M. & Saibil, H. R. (1999). Cryo-electron microscopy structure of an SH3 amyloid fibril and model of the molecular packing. *EMBO J.* **18**, 815–821.
20. Jimenez, J. L., Nettleton, E. J., Bouchard, M., Robinson, C. V., Dobson, C. M. & Saibil, H. R. (2002). The protofilament structure of insulin amyloid fibrils. *Proc. Natl Acad. Sci. USA*, **99**, 9196–9201.
21. Tattum, M. H., Cohen-Krausz, S., Khalili-Shirazi, A., Jackson, G. S., Orlova, E. V., Collinge, J. *et al.* (2006). Elongated oligomers assemble into mammalian PrP amyloid fibrils. *J. Mol. Biol.* **357**, 975–985.
22. Zandomeneghi, G., Krebs, M. R., McCammon, M. G. & Fandrich, M. (2004). FTIR reveals structural differences between native beta-sheet proteins and amyloid fibrils. *Protein Sci.* **13**, 3314–3321.
23. Serpell, L. C., Sunde, M., Benson, M. D., Tennent, G. A., Pepys, M. B. & Fraser, P. E. (2000). The protofilament substructure of amyloid fibrils. *J. Mol. Biol.* **300**, 1033–1039.
24. Whittemore, N. A., Mishra, R., Kheterpal, I., Williams, A. D., Wetzel, R. & Serpersu, E. H. (2005). Hydrogen-deuterium (H/D) exchange mapping of abeta1-40 amyloid fibril secondary structure using nuclear magnetic resonance spectroscopy. *Biochemistry*, **44**, 4434–4441.
25. Kheterpal, I., Williams, A., Murphy, C., Bledsoe, B. & Wetzel, R. (2001). Structural features of the Abeta amyloid fibril elucidated by limited proteolysis. *Biochemistry*, **40**, 11757–11767.
26. Shivaprasad, S. & Wetzel, R. (2004). An intersheet packing interaction in A beta fibrils mapped by disulfide cross-linking. *Biochemistry*, **43**, 15310–15317.
27. Sciarretta, K. L., Gordon, D. J., Petkova, A. T., Tycko, R. & Meredith, S. C. (2005). Abeta40-Lactam(D23/K28) models a conformation highly favorable for nucleation of amyloid. *Biochemistry*, **44**, 6003–6014.
28. Williams, A. D., Portelius, E., Kheterpal, I., Guo, J. T., Cook, K. D., Xu, Y. & Wetzel, R. (2004). Mapping abeta amyloid fibril secondary structure using scanning proline mutagenesis. *J. Mol. Biol.* **335**, 833–842.
29. Dubochet, J., Adrian, M., Chang, J. J., Homo, J. C., Lepault, J., McDowall, A. W. & Schultz, P. (1988). Cryo-electron microscopy of vitrified specimens. *Quart. Rev. Biophys.* **21**, 129–228.
30. Mindell, J. A. & Grigorieff, N. (2003). Accurate determination of local defocus and specimen tilt in electron microscopy. *J. Struct. Biol.* **142**, 334–347.
31. Frank, J., Radermacher, M., Penczek, P., Zhu, J., Li, Y., Ladjadj, M. & Leith, A. (1996). SPIDER and WEB: processing and visualization of images in 3D electron microscopy and related fields. *J. Struct. Biol.* **116**, 190–199.
32. Egelman, E. H. (2000). A robust algorithm for the reconstruction of helical filaments using single-particle methods. *Ultramicroscopy*, **85**, 225–234.
33. Yang, S., Yu, X., Galkin, V. E. & Egelman, E. H. (2003). Issues of resolution and polymorphism in single-particle reconstruction. *J. Struct. Biol.* **144**, 162–171.
34. McRee, D. E. (1999). XtalView/Xfit–A versatile program for manipulating atomic coordinates and electron density. *J. Struct. Biol.* **125**, 156–165.
35. Pettersen, E. F., Goddard, T. D., Huang, C. C., Couch, G. S., Greenblatt, D. M., Meng, E. C. & Ferrin, T. E. (2004). UCSF Chimera–a visualization system for exploratory research and analysis. *J. Comput. Chem.* **25**, 1605–1612.

Edited by F. Schmid

(Received 14 April 2006; received in revised form 8 June 2006; accepted 5 July 2006)